Journal of Circuits, Systems, and Computers
Vol. 26, No. 7 (2017) 1750106 (16 pages)

DOI: 10.1142/S0218126617501067

An Approach to Microcontroller-Based Realization of Boost Converter with Quasi-Sliding Mode Control*

Muhanad Almawlawe[†], Darko Mitić[‡], Dragan Antić[§] and Zoran Icić[¶]

Faculty of Electronic Engineering, University of Niš,
Aleksandra Medvedeva 14, 18000 Niš, Serbia
[†]*muhanadhashim@gmail.com*
[‡]*darko.mitic@elfak.ni.ac.rs*
[§]*dragan.antic@elfak.ni.ac.rs*
[¶]*zoran.icic@elfak.ni.ac.rs*

Received 30 July 2016
Accepted 7 December 2016
Published 26 January 2017

The paper considers a realization of quasi-sliding mode control for DC–DC boost-type converter on ATmega8 microcontroller. The proposed control law represents a combination of discrete-time sliding mode and generalized minimum variance control techniques. The control design is based on input–output converter model and only the sensed output voltage is used for generating control signal. This approach simplifies the practical realization of boost converter since there is no need for current sensors. By introducing an additional discrete-time integrator in control, the converter accuracy in steady-state under load and input voltage variations is enhanced. The experimental prototype is developed and several experiments are conducted to validate the functionalities of the proposed solution. The maximum load and line regulation errors of the proposed converter are 1.55% and 2.9%, respectively.

Keywords: Boost converter; continuous conduction mode; quasi-sliding mode control; generalized minimum variance control; pulse width modulation; digital signal processing.

1. Introduction

The sliding mode (SM) control belongs to the class of nonlinear control known as variable structure control.[1–3] It forces system state to slide along predefined surface providing system robustness to parameter variations and external disturbances, even invariance[4] for systems satisfying matching conditions. These SM control properties recommend it for DC–DC converting applications under load variations. However, SM control operates at varying switching frequency causing inductor and transformer core losses, as well as producing some EMI noise issues. This problem can be overcome

*This paper was recommended by Regional Editor Zoran Stamenkovic.
[‡]Corresponding author.

by using a control based on pulse-width-modulation (PWM) fixed-frequency techniques, also known as a duty cycle control.[5] It has been proven[6] that the system dynamics with SM controller is equivalent to the system dynamics with PWM controller, i.e., the SM equivalent control[4,1] u_{eq} is equal to the duty cycle control signal d.

The implementation of PWM techniques in control of DC–DC boost-type converter operating in continuous conduction mode (CCM) may cause the appearance of right-half-plane-zero (RHPZ) in its duty-cycle-to-output-voltage transfer function, obtained on the basis of the state-space average model[7,8] of converter. This makes the design of boost converter voltage controller more difficult and limits the system bandwidth.[9] In recent years, several boost converters with PWM-based SM control have been developed. A unified approach to design of PWM-based SM voltage controller for three basic converters (buck, boost and buck–boost) is demonstrated in Ref. 10. The fixed-frequency SM current controller for boost converter is considered in Ref. 11. In order to increase the steady-state accuracy of boost converter, an additional double-integral term of the controlled variables is introduced in the sliding surface equation of indirect SM controllers.[12] Based on the similar state-space model of boost converter as in the previous works,[10–12] the proportional plus integral (PI) type of switching (sliding) function is introduced in Ref. 13 to cope with load variations. Moreover, the switching function parameter is tuned as per a load, resulting in adaptive unlike conventional SM control. The fast terminal SM control, having a nonlinear switching function to guarantee finite-time convergence to sliding surface, is implemented in the output voltage control of boost converter.[14] The proposed control scheme combines finite-time and exponent convergent properties in design of switching function, in order to improve the convergence performance if the system state is far from the equilibrium point.

Boost converters are widely used as power stages in renewable energy resources such as photovoltaic (PV) systems. The connection of these systems to a main DC bus via power converters enables high maximum power point tracking (MPPT). Thanks to the fact that the input impedance of boost converter can be tuned by duty cycle, i.e., it can be considered as an adjustable loss-free resistor (LFR), the operating point of PV system can be changed in order to maximize the output power. An overview of MPPT techniques for PV power systems is presented in Ref. 15. Many MPPT methods do not take into account the system uncertainties and are not robust to them. To cope with parameter perturbation, MPPT algorithms with SM control are proposed for eliminating the perturbation effects.[16,17] In Ref. 18 MPP curve is approximated, taking into account not only the voltage and current on the PV panel, but also the temperature. This linear approximation is used then to form a switching function of SM controller. The impedance matching can be also obtained by the cascade connection of two boost converters driven by SM controllers based on LFR concept.[19]

The fixed switching frequency of SM control can be attained by using discrete-time SM controllers.[20–22] However, the discretization process of SM control causes the quasi-sliding motion[23] in the vicinity of sliding surface and produces an undesirable chattering. The latter phenomenon is also present in boost converters with PWM-based continuous-time SM control techniques. It can be suppressed by using the boundary layer approach,[17] the chattering-free[14,16] control methods or, recently, the tensor product model[24] for sliding surface design.[25]

One of the first approaches in design of discrete-time SM-like controller is considered in Ref. 26 for the control of DC–DC buck converter. The control algorithm is implemented as a fuzzy logic controller with sliding mode-like characteristics. Discrete-time SM controllers for boost converter[27,28] can be designed based on its state-space average model, which is the nonminimum phase system if the output voltage is directly controlled. Therefore, the indirect method is used that controls the inductor current, whose reference signal is selected such that a desired output voltage is obtained. The choice of inductor current, as an output, results in minimum phase system, but the problem of output voltage convergence to its reference signal arises. In Ref. 27, the design of discrete-time SM control with reference model is presented. The cascade regulation scheme, consisting of the inner inductor current loop with discrete-time SM control and the outer one being composed of a discrete-time PI controller for output voltage regulation, is considered in Ref. 28. Another approach to modeling of boost converter,[29,30] using discrete Lagrange–Euler equations, results also in nonminimum phase system. The main difficulty to stabilize the unstable inductor current variable and to provide an output voltage that tracks a desired reference signal is addressed in these papers. Due to unstable zero dynamics of state-space average model, the implementation of discrete-time SM control using stable system center[31] in direct control of the output voltage may be considered as a promising solution to this problem.

All previous control design techniques are based on the state-space model representation of boost converter and, therefore, the measuring of inductor current is mandatory. In this paper, we present a discrete-time SM control, designed by using the input–output model of boost converter in the form of a discrete-time transfer function, which eliminates the need for additional current sensor. The proposed quasi-sliding mode (QSM) control represents the combination of generalized minimum variance (GMV) and discrete-time SM control techniques.[32,33] GMV control is suggested herein to cope with RHPZ of duty-cycle-to-output-voltage transfer function and to enable the controller design based only on converter output voltage measuring. In order to alleviate chattering and achieve better converter accuracy, the discrete-time SM control component is filtered through discrete-time integrator.[32] The theoretical background of the proposed control for the boost converter is given in Ref. 34, based on contributions presented in Ref. 33 and partially in Ref. 32. However, due to parameter variations, some additional stability issues are considered in this paper, extending the theoretical results in that way. Similar QSM controller is implemented in voltage control of buck converter.[35] As the buck converter represents a minimum phase system, the discrete-time SM control is combined with the minimum variance (MV) control.

Traditionally, digital signal processors are used to implement controllers for power converters. In recent years, some research efforts are dedicated to design of low-cost solutions for the voltage control of boost converter. In Ref. 36, the sliding-mode hysteretic control algorithm, based on state-space model, is realized on low-cost memory hardware. The sliding surface is derived in advance and stored in memory lookup table, whose output drives a boost converter power switch. The continuous-time SM control, designed by using state-space average model, is digitally implemented using low-cost dsPIC30F4013 microcontroller with small computing power.[37] The selection of sliding surface provides the current mode controller, making the inductor current a function of the output voltage. In this paper, we demonstrate how the proposed QSM control for boost converter can be realized on widely used ATmega8 microcontroller. It is shown that this control is simple enough to be easily implemented on standard 8-bit microcontrollers, but at the expense of little lower accuracy and slower dynamical response. Moreover, the proposed boost converter realization gives satisfactory experimental results, indicating that better results can be expected if digital signal processor is used.

The paper is organized as follows. In Sec. 2, the modeling of boost converter is considered. The brief design procedure of proposed QSM control algorithm is given in Sec. 3. The experimental setup is presented and the experimental results are discussed in Sec. 4. Section 5 contains some concluding remarks.

2. Boost Converter Modeling

Mathematical models of the boost converter provide the pathway to various control strategies discussed in literature. In this paper, the model of boost converter is given in the form of discrete-time transfer function, derived from the state-space model.[10] The schematic diagram of boost converter with the proposed QSM controller is shown in Fig. 1. Herein, C_k, L and R_L represent the capacitance, inductance and load resistance of the converter, respectively; i_c, i_L and i_{out} are the capacitor, inductor and output (load) currents, respectively; V_{ref}, v_{in} and v_{out} denote the reference, input, and output voltages, respectively; β denotes sensor gain, whereas u representing the signal driving the power switch S_w. The boost converter operating in CCM is considered in modeling process. By taking the output voltage and its time-derivative for the state coordinates ($x_1 = v_{\mathrm{out}}, x_2 = dv_{\mathrm{out}}/dt$), the linearized small-signal state-space model of boost converter in continuous-time domain can be written in the following form[10]:

$$\begin{aligned} \dot{x}(t) &= \begin{bmatrix} 0 & 1 \\ 0 & -\dfrac{1}{R_L C_k} \end{bmatrix} x(t) + \begin{bmatrix} 0 \\ \dfrac{V_{\mathrm{in}} - V_{\mathrm{out}}}{LC_k} \end{bmatrix} u(t)\,, \\ y(t) &= [\,\beta \quad 0\,]x(t)\,, \end{aligned} \tag{1}$$

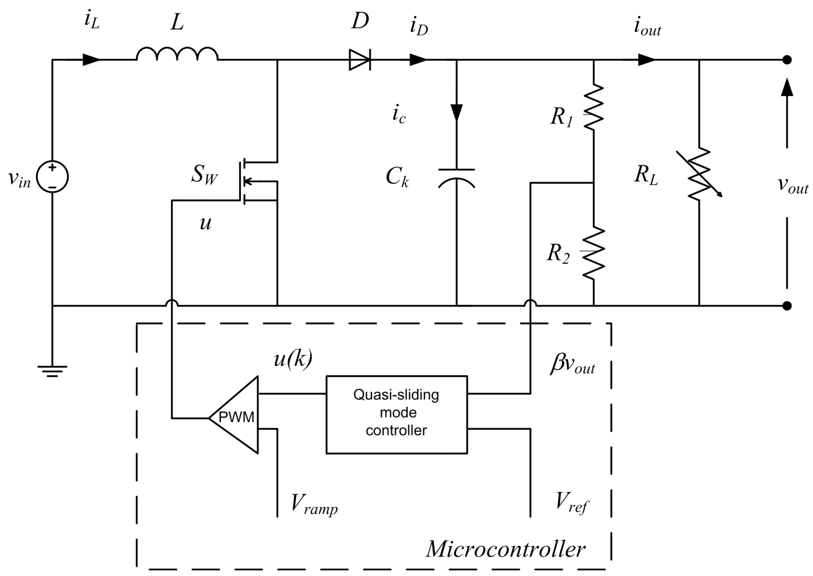

Fig. 1. Boost converter with QSM controller.

where V_{in} and V_{out} are the nominal values of boost converter input and output voltages.

The transfer function of boost converter can be derived directly from Eq. (1) as

$$W_{\text{boost}}(s) = \frac{Y(s)}{U(s)} = \frac{\dfrac{\beta(V_{\text{in}} - V_{\text{out}})}{LC}}{s^2 + \dfrac{1}{R_L C} s} \,. \tag{2}$$

Under the assumption that control signal is constant during the sampling period T, $u(t) = u(kT)$, $kT < t < (k+1)T$, the input–output model of boost converter in z-domain is given by

$$y(k) = \frac{z^{-1} B(z^{-1})}{A(z^{-1})} u(k) \,, \tag{3}$$

where z^{-1} is the unit delay, i.e., $z^{-1} = e^{-sT}$, s denotes a complex variable, $\bullet(k) = \bullet(kT)$ and

$$\begin{aligned} A(z^{-1}) &= A_n(z^{-1}) + \Delta A(z^{-1}) \,, \\ B(z^{-1}) &= B_n(z^{-1}) + \Delta B(z^{-1}) \,, \end{aligned} \tag{4}$$

$A_n(z^{-1}), B_n(z^{-1})$, $\Delta A(z^{-1})$ and $\Delta B(z^{-1})$ represent the polynomials with nominal and perturbed values of boost converter parameters, respectively.

3. QSM Control Law

The main aim of control design is to maintain the sensed output voltage $y(k) = \beta v_{\text{out}}(k)$ as stable, constant and equal to some reference voltage $V_r(k) = V_{\text{ref}}$, despite the variations of load resistance R_L and input voltage v_{in}. In order to achieve the design task, QSM control algorithm[32,33] is used to control boost converter. It is defined by

$$u(k) = -\frac{F(z^{-1})y(k) - C(z^{-1})V_r(k+1) + \dfrac{\alpha T}{1 - z^{-1}}\text{sgn}(s(k))}{E(z^{-1})B_n(z^{-1}) + Q(z^{-1})}\,, \tag{5}$$

where $s(k)$ represents the switching function given by

$$s(k+1) = C(z^{-1})(y(k+1) - V_r(k+1)) + Q(z^{-1})u(k)\,, \tag{6}$$

$C(z^{-1})$ is a polynomial with all zeros inside the unit disk of z-plane, and $Q(1) = 0$. $E(z^{-1})$ and $F(z^{-1})$ are solutions of the so-called Diophantine equation:

$$C(z^{-1}) = E(z^{-1})A_n(z^{-1}) + z^{-1}F(z^{-1})\,, \tag{7}$$

$s(k) = 0$ is an equation of sliding surface in general case. The closed-loop dynamics is directly derived from Eqs. (3) and (6) in the form of [32]:

$$y(k) = \frac{B(z^{-1})(C(z^{-1})V_r(k) + s(k))}{B(z^{-1})C(z^{-1}) + A(z^{-1})Q(z^{-1})}\,, \tag{8}$$

It is obvious from Eq. (8) that, in order to guarantee the system stability, all roots of the equation $B(z^{-1})C(z^{-1}) + A(z^{-1})Q(z^{-1}) = 0$ should be inside the unit disk in the z-plane, and the pairs $(B(z^{-1}),\ Q(z^{-1}))$,$(C(z^{-1}),\ A(z^{-1}))$ and $(C(z^{-1}),\ Q(z^{-1}))$ should not have common zeroes outside this disk. The system steady-state accuracy can be obtained from Eq. (8) for $z = 1$ and $Q(1) = 0$ as

$$y(\infty) = V_r(\infty) + \frac{1}{C(1)}s(\infty)\,. \tag{9}$$

Substituting Eq. (5) in Eq. (3), taking into account Eqs. (4), (6) and (7), one gets

$$B(z^{-1})s(k+1) = -\frac{\alpha TB(z^{-1})\text{sgn}(s(k))}{1 - z^{-1}} + E(z^{-1})P(z^{-1})y(k+1)\,, \tag{10}$$

where $P(z^{-1}) = A_n(z^{-1})\Delta B(z^{-1}) - B_n(z^{-1})\Delta A(z^{-1})$. Replacing $y(k+1)$ in Eq. (10) by Eq. (8), having in mind that $V_r(k+1) = V_r(k) = V_{\text{ref}} = \text{const.}$, gives:

$$\Delta s(k+1) = -\frac{B(z^{-1})C(z^{-1}) + A(z^{-1})Q(z^{-1})}{B(z^{-1})C(z^{-1}) + A(z^{-1})Q(z^{-1}) - E(z^{-1})P(z^{-1})}\alpha T\,\text{sgn}(s(k))\,, \tag{11}$$

where $\Delta s(k+1) = s(k+1) - s(k)$ is bounded if all roots of the equation $B(z^{-1})C(z^{-1}) + A(z^{-1})Q(z^{-1}) - E(z^{-1})P(z^{-1}) = 0$ are inside the unit disk in the z-plane.

The latter is accomplished by the appropriate selection of the polynomials $C(z^{-1})$ and $Q(z^{-1})$. Finally, the switching function dynamics is defined as

$$s(k+1) = s(k) - \alpha T \mathrm{sgn}(s(k)) + l(k+1)\,, \tag{12}$$

with

$$l(k) = \frac{E(z^{-1})P(z^{-1})}{B(z^{-1})C(z^{-1}) + A(z^{-1})Q(z^{-1})}\Delta s(k)\,, \tag{13}$$

including all parameter perturbations and, obviously, $|l(k)| \leq \Lambda$, where Λ is a positive real constant. If $\alpha > \Lambda/T$, a quasi-sliding motion is established in Δ-vicinity of $s(k) = 0$, i.e., $|s(k)| \leq \Delta$ is always satisfied, where Δ is a function of αT. The proof of this statement is beyond the scope of this paper, and can be found in Ref. 35.

4. Experimental Prototype and Results

The verification of proposed boost converter is presented in this section. The developed experimental prototype is depicted in Fig. 2, whereas the scheme of microcontroller based boost converter is given in Fig. 3. Table 1 contains the nominal values of converter parameters. With $T = 1\,\mathrm{ms}$, the discrete-time model (Eq. (3)) is defined by $A(z^{-1}) = 1 - 1.9802z^{-1} + 0.9802z^{-2}$ and $B(z^{-1}) = 1.3515 - 1.3425z^{-1}$. Then, the parameters of QSM controller are selected and calculated as: $C(z^{-1}) = 1 - 1.067z^{-1} + 0.2846z^{-2}$, $Q(z^{-1}) = 0.05(1 - z^{-1})$, $E(z^{-1}) = 1$, $F(z^{-1}) = 0.9132 - 0.6956z^{-1}$ and $\alpha = 10$.

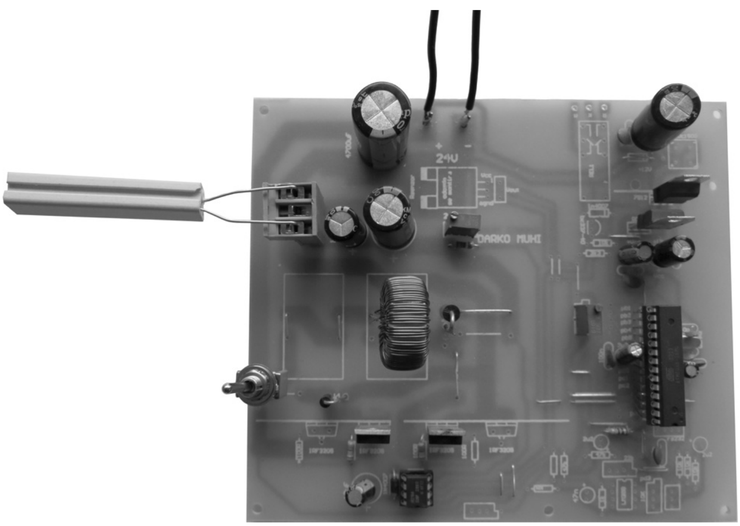

Fig. 2. Experimental prototype of the proposed boost converter.

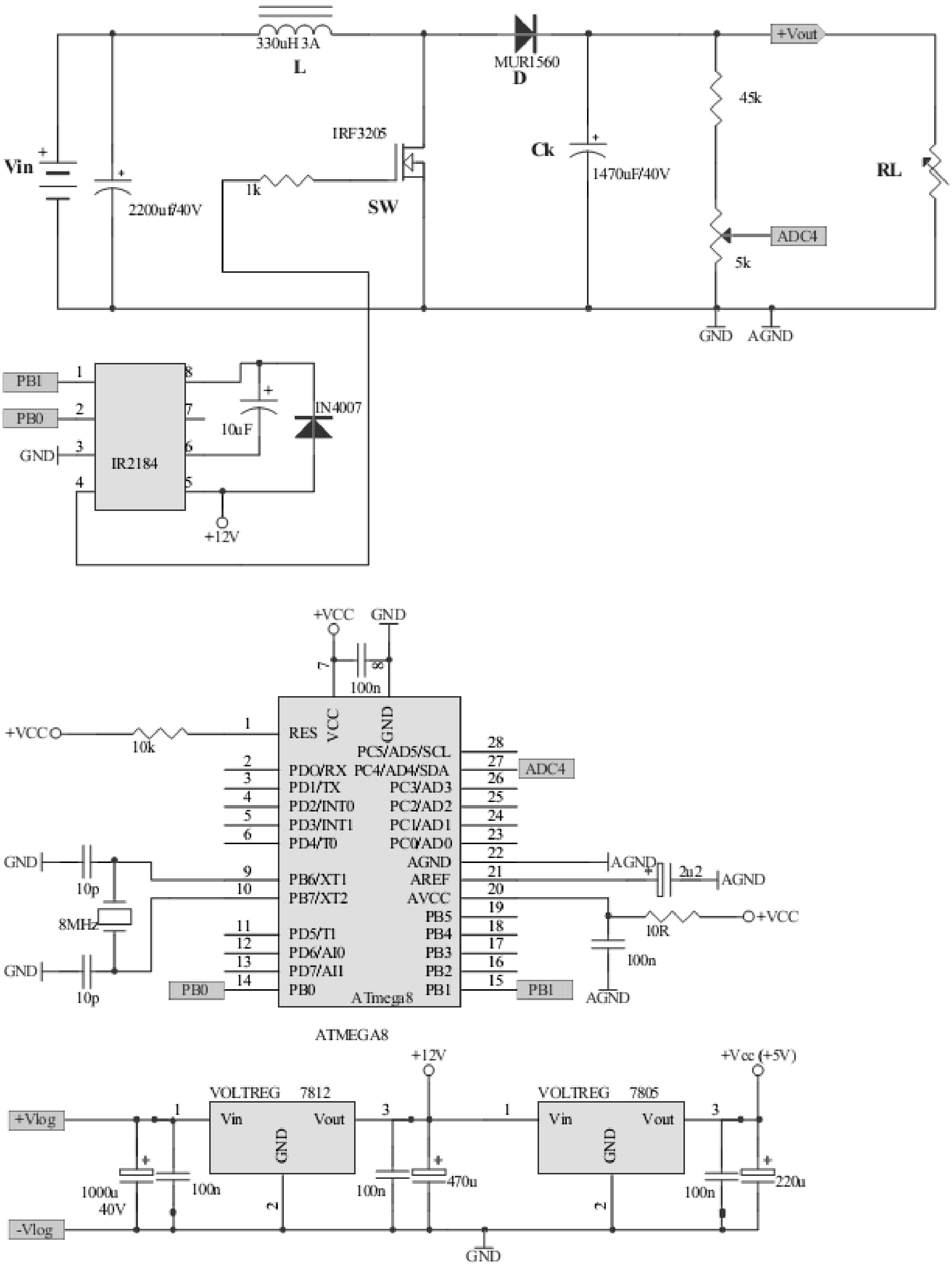

Fig. 3. Scheme of boost converter realization with ATmega8 microcontroller.

Table 1. Boost converter parameter values.

Description	Parameter	Nominal Value
Input voltage	V_{in}	12 V
Desired output voltage	V_{out}	24 V
Capacitance	C_k	1,470 μF
Inductance	L	330 μH
PWM frequency	f_{pwm}	7.874 kHz
Sampling period	T	1 ms
Minimum load resistance	R_{L_min}	22.67 Ω
Maximum load resistance	R_{L_max}	68 Ω

QSM control algorithm is realized by using 8-bit microcontroller ATmega8.[38] The sensed output voltage is fed into its 10-bit A/D converter. PWM is also incorporated in microcontroller with the switching frequency $f_{pwm} = 7.874$ kHz. Thanks to such choice of f_{pwm}, the influence of RHPZ in duty-cycle-to-output-voltage transfer functions is significantly suppressed but at the cost of lower bandwidth.[7]

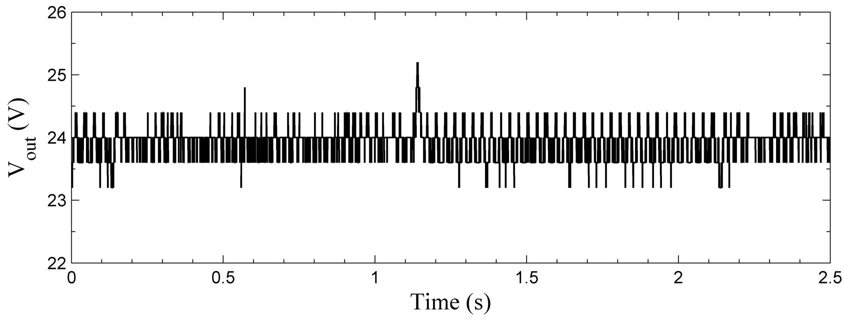

(a)

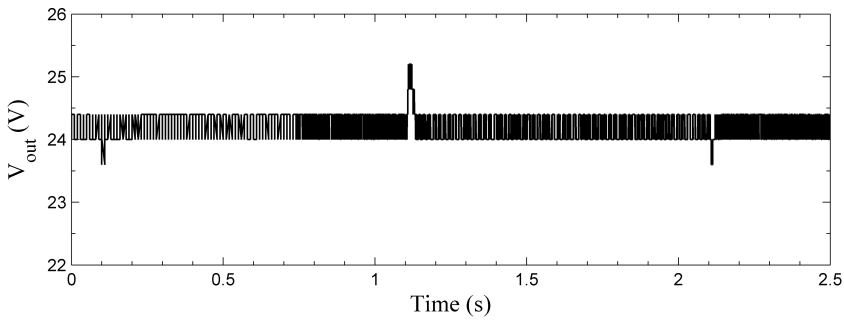

(b)

Fig. 4. Experimental waveforms of v_{out} (panels (a)–(c)) and i_{out} (panel (d)) of the boost converter with QSM control, alternating between load resistances 68 Ω and 34 Ω and operating at (a) $V_{in} = 10.5$ V, (b) $V_{in} = 12$ V and (c) $V_{in} = 13.5$ V.

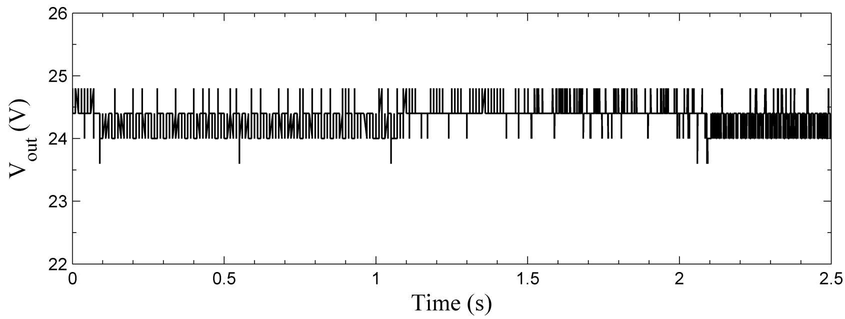

(c)

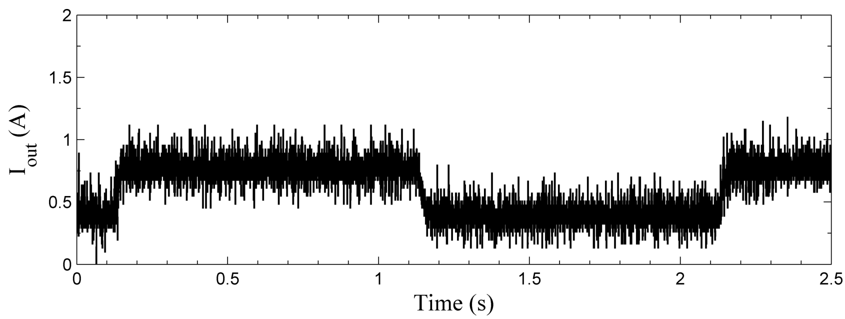

(d)

Fig. 4. (*Continued*)

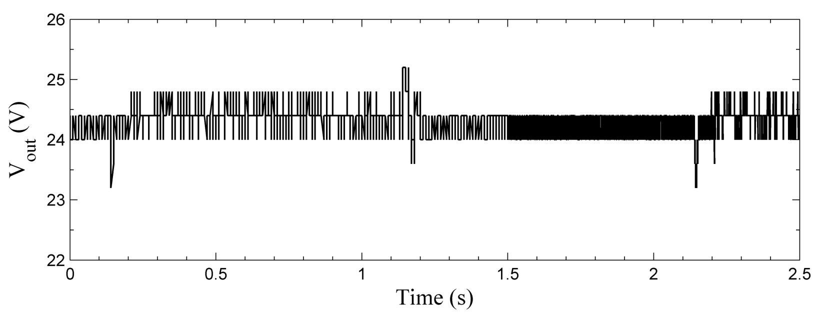

(a)

Fig. 5. Experimental waveforms of v_{out} (panels (a)–(c)) and i_{out} (panel (d)) of the boost converter with QSM control, alternating between load resistances $34\,\Omega$ and $22.67\,\Omega$ and operating at (a) $V_{\text{in}} = 10.5\,\text{V}$, (b) $V_{\text{in}} = 12\,\text{V}$ and (c) $V_{\text{in}} = 13.5\,\text{V}$.

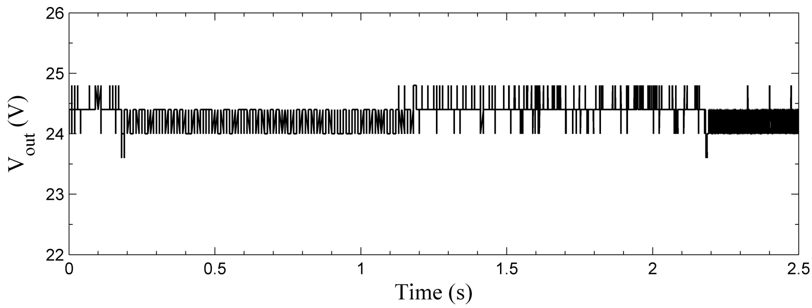

(b)

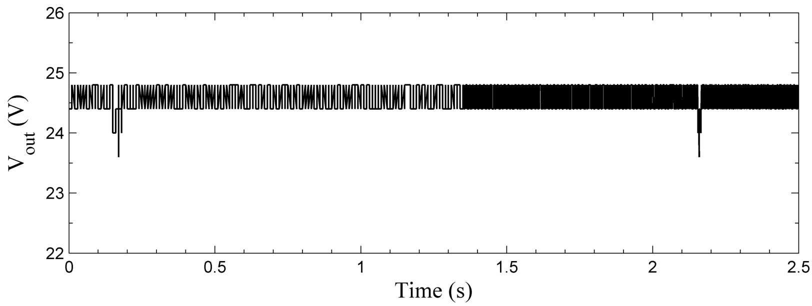

(c)

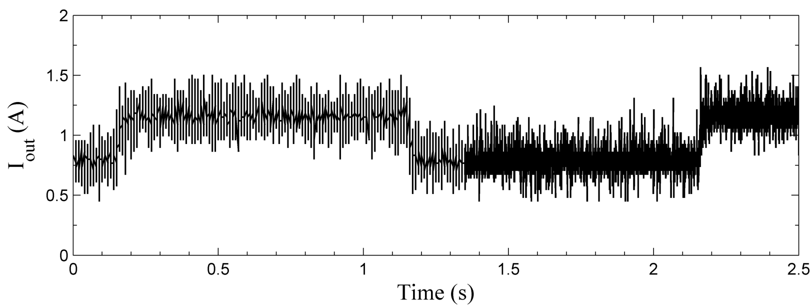

(d)

Fig. 5. (*Continued*)

In order to analyze load and line regulation properties of the realized microcontroller based boost converter with QSM control, the step load changes from $R_L = 68\,\Omega$ to $R_L = 34\,\Omega$, from $R_L = 34\,\Omega$ to $R_L = 22.67\,\Omega$ and from $R_L = 68\,\Omega$ to $R_L = 22.67\,\Omega$ are applied at three different input voltage values: minimum ($V_{\text{in}} = 10.5\,\text{V}$), nominal ($V_{\text{in}} = 12\,\text{V}$) and maximum ($V_{\text{in}} = 13.5\,\text{V}$). The experimental results in the form of output voltage v_{out} and current i_{out} waveforms are presented in Figs. (4)–(6).

According to Table 2, maximum load regulation error occurs at $V_{\text{in}} = 10.5\,\text{V}$ with deviation of 1.55% from V_{out} at nominal condition. On the other hand, the maximum line regulation error is at maximum load ($R_L = 22.67\,\Omega$) with deviation of 2.9% from

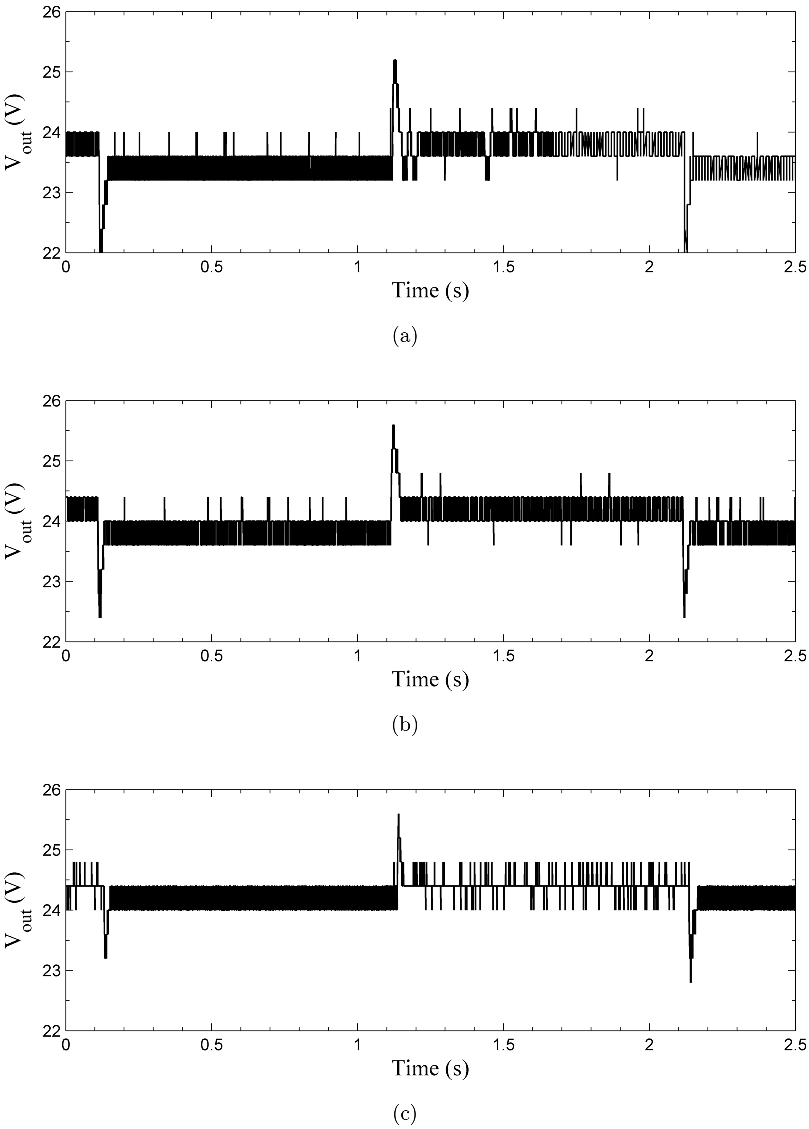

Fig. 6. Experimental waveforms of v_{out} (panels (a)–(c)) and i_{out} (panel (d)) of the boost converter with QSM control, alternating between load resistances $68\,\Omega$ and $22.67\,\Omega$ and operating at (a) $V_{\text{in}} = 10.5\,\text{V}$, (b) $V_{\text{in}} = 12\,\text{V}$ and (c) $V_{\text{in}} = 13.5\,\text{V}$.

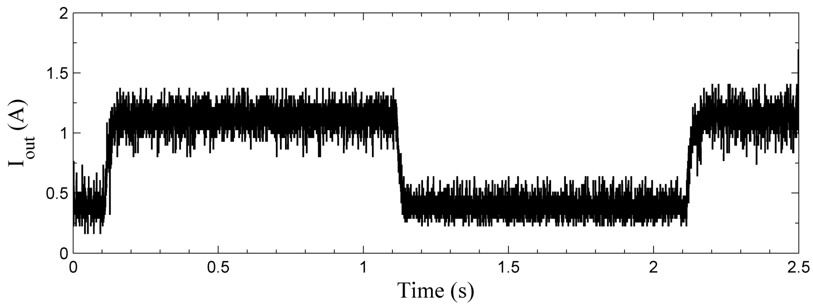

(d)

Fig. 6. (*Continued*)

Table 2. Load regulation property ($V_{\text{out (nominal condition)}} = 23.9\,\text{V}$ at $V_{\text{in}} = 12\,\text{V}$ and $R_{\text{L\_min}} = 22.67\,\Omega$).

V_{in}	$\Delta V_{\text{out}} = V_{\text{out}(68\,\Omega)} - V_{\text{out}(22.67\,\Omega)}$	$\dfrac{\Delta V_{\text{out}}}{V_{\text{out(nominal condition)}}} \times 100\%$
10.5 V	0.37 V	1.55% of $V_{\text{out (nominal condition)}}$
12 V	0.32 V	1.32% of $V_{\text{out (nominal condition)}}$
13.5 V	0.21 V	0.89% of $V_{\text{out (nominal condition)}}$

Table 3. Line regulation property ($V_{\text{out (nominal condition)}} = 23.9\,\text{V}$ at $V_{\text{in}} = 12\,\text{V}$ and $R_{\text{L\_min}} = 22.67\,\Omega$).

Loading condition	$\Delta V_{\text{out}} = V_{\text{out}(V\text{in}=13.5\,\text{V})} - V_{\text{out}(V\text{in}=10.5\,\text{V})}$	$\dfrac{\Delta V_{\text{out}}}{V_{\text{out(nominal condition)}}} \times 100\%$
$R_{\text{L\_max}} = 68\,\Omega$	0.4 V	1.67% of $V_{\text{out (nominal condition)}}$
$R_{\text{L\_medium}} = 34\,\Omega$	0.3 V	1.25% of $V_{\text{out (nominal condition)}}$
$R_{\text{L\_min}} = 22.67\,\Omega$	0.7 V	2.9 % of $V_{\text{out (nominal condition)}}$

V_{out} at nominal condition (see Table 3). It is worth noting that the load and line regulation properties depend largely on microcontroller's A/D converter and PWM resolution, as well as on the choice of QSM controller parameters $C(z^{-1})$, α and T. Theoretically, according to Eq. (9), the converter steady-state error should be approximately 400 mV. Therefore, a better accuracy may be expected if a faster microcontroller with better A/D converter and PWM resolution is used.

5. Conclusion

In this paper, the quasi-sliding mode control for DC–DC boost-type converter is discussed, and its realization on 8-bit ATmega8 microcontroller is presented.

The proposed control is a combination of discrete-time sliding mode control and generalized minimum variance control, and can be implemented by measuring only converter output voltage without the need for additional current sensors. The experimental prototype is developed and several tests are carried out. The experimental results demonstrate good regulation performances under load and input voltage variations, in spite of low resolution of A/D converter and PWM. Better results may be expected with faster digital signal processors. It can be concluded that the proposed boost converter with quasi-sliding mode control is feasible by using standard 8-bit microcontrollers.

Acknowledgments

This paper was realized as a part of the Projects III 43007 and TR 35005 financed by the Ministry of Education, Science and Technological Development of the Republic of Serbia.

References

1. V. I. Utkin, *Sliding Modes and Their Applications in Variable Structure Systems* (Mir, Moscow, 1978).
2. J. Y. Hung, W. Gao and J. C. Hung, Variable structure control: A survey, *IEEE Trans. Ind. Electron.* **40**(1993) 2–21.
3. C. Edwards and S.-K. Spurgeon, *Sliding Mode Control: Theory and Application* (Taylor and Francis, London, 1998).
4. B. Draženović, The invariance conditions in variable structure systems, *Automatica* **5** (1969) 287–295.
5. S.-C. Tan, Y. M. Lai, C. K. Tse and M. K. H. Cheung, A fixed-frequency pulse-width modulation based quasi-sliding-mode controller for buck converters, *IEEE Trans. Power Electron.* **20** (2005) 1379–1392.
6. H. Sira-Ramirez, A geometric approach to pulse width modulated control in nonlinear dynamical systems, *IEEE Trans. Autom. Control* **34** (1989) 184–187.
7. C. Basso, Understanding the right-half-plane zero — Analytical description of the right-half-plane zero for voltage-mode and current-mode converters (2009), http://power-electronics.com/power-management/understanding-right-half-plane-zero.
8. K. Wu, *Power Converters with Digital Filter Feedback Control* (Elsevier, 2016).
9. V. Utkin, Sliding mode control of DC–DC converters, *J. Franklin Inst.* **350** (2013) 2146–2165.
10. S. C. Tan, Y. M. Lai and C. K. Tse, A unified approach to the design of PWM-based sliding-mode voltage controllers for basic dc–dc converters in continuous conduction mode, *IEEE Trans. Circuits Syst.* **53** (2006) 1816–1827.
11. S. C. Tan, Y. M. Lai, C. K. Tse, L. Martínez-Salamero and C. K. Wu, A fast-response sliding-mode controller for boost-type converters with a wide range of operating conditions, *IEEE Trans. Ind. Electron.* **54** (2007) 3276–3286.
12. S. C. Tan, Y. M. Lai and C. K. Tse, Indirect sliding mode control of power converters via double integral sliding surface, *IEEE Trans. Power Electron.* **23** (2008) 600–611.

13. A. J. Mehta and B. B. Naik, Adaptive sliding mode controller with modified sliding function for DC–DC boost converter, *Proc. 2014 IEEE Int. Conf. Power Electronics, Drives and Energy Systems (PEDES)* (2014), pp. 340–345.
14. I. Yazici and E. K. Yaylaci, Fast and robust voltage control of DC–DC boost converter by using fast terminal sliding mode controller, *IET Power Electron.* **9** (2016) 120–125.
15. B. Subudhi and R. Pradhan, A comparative study on maximum power point tracking techniques for photovoltaic power systems, *IEEE Trans. Sustain. Energy* **4** (2013) 89–98.
16. M. R. Mojallizadeh, M. Badamchizadeh, S. Khanmohammadi and M. Sabahi, Designing a new robust sliding mode controller for maximum power point tracking of photovoltaic cells, *Sol. Energy* **132** (2016) 538–546.
17. R. Pradhan and B. Subudhi, Double integral sliding mode MPPT control of a photovoltaic system, *IEEE Trans. Control Syst. Technol.* **24** (2016) 285–292.
18. N. Vázquez, Y. Azaf, I. Cervantes, E. Vázquez and C. Hernández, Maximum power point tracking based on sliding mode control, *Int. J. Photoenergy* **2015** (2015) 380684.
19. R. Haroun, A. E. Aroudi, A. Cid-Pastor, G. Garcia, C. Olalla and L. Martınez-Salamero, Impedance matching in photovoltaic systems using cascaded boost converters and sliding-mode control, *IEEE Trans. Power Electron.* **30** (2015) 3185–3199.
20. W. B. Gao, Y. Wang and A. Homaifa, Discrete-time variable structure control system, *IEEE Trans. Ind. Electron.* **42** (1995) 117–122.
21. A. Bartoszewicz, Discrete-time quasi-sliding-mode control strategies, *IEEE Trans. Ind. Electron.* **45** (1998) 633–637.
22. Č. Milosavljević, Discrete-time VSS, *Variable Structure Systems: From Principles to Implementation*, eds. A. Šabanović, L. Fridman and S. Spurgeon, IEE Control Engineering Series, Vol. 66 (MPG Books, 2004), pp. 99–129.
23. Č. Milosavljević, General conditions of the existence of a quasi-sliding mode on the switching hyperplane in discrete variable structure systems, *Autom. Remote Control* **46** (1985) 307–314.
24. R.-E. Precup, C.-A. Dragos, S. Preitl, M.-B. Radac and E. M. Petriu, Novel tensor product models for automatic transmission system control, *IEEE Syst. J.* **6** (2012) 488–498.
25. P. Korondi, Tensor product model transformation-based sliding surface design, *Acta Polytech. Hung.* **3** (2006) 23–35.
26. A. G. Perry, G. Feng, Y.-F. Liu and P. C. Sen, A new sliding mode like control method for buck converter, *Proc. 35th Annu. IEEE Power Electronics Specialists Conf.* (2004), pp. 3688–3693.
27. I. Yazici, Robust voltage-mode controller for DC–DC boost converter, *IET Power Electron.* **8** (2015) 342–349.
28. E. Vidal-Idiarte, A. Marcos-Pastor, G. Garcia, A. Cid-Pastor and L. Martinez-Salamero, Discrete-time sliding-mode-based digital pulse width modulation control of a boost converter, *IET Power Electron.* **8** (2015) 708–714.
29. J. Rivera, F. Chavira and A. Loukianov, On the discrete-time modeling of a DC-to-DC power converter and control design with discrete-time sliding modes, *Math. Probl. Eng.* **2013** (2013) 460281.
30. J. Rivera, F. Chavira, A. Loukianov, S. Ortega and J. J. Raygoza, Discrete-time modeling and control of a boost converter by means of a variational integrator and sliding modes, *J. Franklin Inst.* **351** (2014) 315–339.
31. O. Iskrenović-Momčilović, Č. Milosavljević and Y. B. Shtessel, Discrete-time variable structure control for causal nonminimum phase systems using stable system center, *Proc. 2006 Int. Workshop Variable Structure Systems* (2006), pp. 45–50.

32. D. Mitić and Č. Milosavljević, Sliding mode based minimum variance and generalized minimum variance controls with $O(T^2)$ and $O(T^3)$ accuracy, *Electr. Eng.* **86** (2004) 229–237.
33. D. Mitić, Digital variable structure systems based on input–output model, Ph.D. thesis, University of Niš, Faculty of Electronic Engineering (2006).
34. M. D. Almawlawe, D. Mitić and M. Milojević, The usage of the digital controller in regulating boost converter, *Circuits Syst.* **6** (2015) 268–279.
35. D. Mitić, D. Antić, M. Milojković, S. Nikolić and S. Perić, Input–output based quasi-sliding mode control of dc–dc converter, *FUElectEnerg* **25** (2012) 69–80.
36. B. Banerjee, R. M. Kotecha and W. W. Weaver, Digital memory look-up based implementation of sliding mode control for dc–dc converters, *Control Eng. Pract.* **54** (2016) 1–11.
37. D. Cortes, D. Navarro, A. Barajas and I. Araujo, Sliding-mode control of power converters feasible to be implemented with low-cost micro controllers, *J. Control Eng. Appl. Inf.* **15** (2013) 3–10.
38. Atmel, 8-Bit Atmel with 8kBytes in-system programmable flash (2013), http://www.atmel.com/images/atme l-2486-8-bit-avr-microcontroller-atmega8_l_datasheet.pdf.